Seismic stratigraphy, structure and morphology of Makarov Basin and surrounding regions: tectonic implications

John Evangelatos [a,*], David C. Mosher [b,1]

[a] Department of Earth Sciences, Dalhousie University, 1355 Oxford Street, Halifax, NS B3H 4J1, Canada
[b] Geological Survey of Canada (Atlantic), Natural Resources Canada, Bedford Institute of Oceanography, 1 Challenger Drive, Dartmouth, NS B2Y 4A2, Canada

ARTICLE INFO

ABSTRACT

The tectonic history of Amerasia Basin, Arctic Ocean, is not well known because of a paucity of data and complexities introduced by the Alpha–Mendeleev Ridge large igneous province. Makarov Basin, at the northern limit of Amerasia Basin and adjacent to Lomonosov Ridge, may provide a window into understanding the larger tectonic framework. The objective of this study is to decipher the sedimentary and tectonic history of northern Amerasia Basin by analysing the seismic stratigraphy, structure and morphology of Makarov Basin and surrounding regions (Alpha and Lomonosov ridges) of the central Arctic Ocean. The principal data sources for this study are a 400 km long multi-channel seismic line, extending from Alpha Ridge to the crest of Lomonosov Ridge via central Makarov Basin, and the Arctic bathymetric chart.

The seismic record within Makarov Basin is divided into five seismic units. The first unit overlying basement hosts Late Cretaceous (minimum age) slope to base of slope sediments. Some of these sediments are interbedded with volcanic or volcanoclastic rocks with a minimum age of 89 Ma. Makarov Basin becomes isolated from proximal sources of sediments after the onset of rifting that separated Lomonosov Ridge from the Barents Shelf, which may have occurred as early as the mid-Late Cretaceous, and led to the creation of Eurasia Basin. Sediments are largely pelagic to hemipelagic as a result of this isolation. This deposition style also applies to the draped sedimentary strata on Alpha and Lomonosov ridges. The uppermost seismic units within Makarov Basin are jump-correlated to the stratigraphic record of the ACEX drill site on top of Lomonosov Ridge to provide age control. This correlation shows that the 44.4–18.2 Ma hiatus documented in the drill core is not apparent in the basin. Inter-ridge correlations and the absence of an obvious planate surface on Alpha Ridge also suggest that sedimentation was uninterrupted on this ridge during the hiatus.

Seismic data reveal a deep subbasin (~5 km thick) within Makarov Basin. This subbasin is immediately adjacent to Lomonosov Ridge within major bends in the general strike orientation of the ridge. The rhomboid shape of the deep subbasin, the straight and steep morphology of the Amerasian flank of Lomonosov Ridge and the presence of numerous sub-parallel ridges (e.g. Geophysicists and Marvin spurs) created by splay faulting are evidence of strike-slip (transtensional) tectonics. This interpretation supports the "rotational" model of opening of Amerasia Basin with a transform to transtensional margin at Lomonosov Ridge. As spreading continued, however, the tectonics became increasingly extensional perpendicular to Lomonosov Ridge. There is no evidence of major tectonic deformation in Makarov Basin beyond the late Paleocene.

© 2016 Elsevier B.V. All rights reserved.

1. Introduction

The Arctic Ocean is the smallest and shallowest of the world's five major oceans. It comprises extensive shallow continental shelves and two major deep-water basins — the Amerasia and Eurasia basins (Fig. 1). The two basins are separated by the Lomonosov Ridge, spanning the Arctic Ocean from the North American shelf off of Ellesmere Island and Northwest Greenland to the East Siberian Shelf. The onset of rifting between Lomonosov Ridge and the Barents Shelf may have commenced as early as the mid-Late Cretaceous (Drachev, 2011), and led to seafloor spreading in Eurasia Basin during the late Paleocene (magnetic chron anomaly 25 or 24; Vogt et al., 1979; Srivastava, 1985; Brozena et al., 2003). Amerasia Basin lies on the opposite side of Lomonosov Ridge. This ridge, Arctic Alaska, Siberia and the Canadian Arctic Archipelago surround the basin (Fig. 1). Prominent geomorphological features within Amerasia Basin include Canada Basin, the Chukchi Borderland, the Alpha and Mendeleev ridges, and the Makarov and Podvodnikov basins (Rowley and Lottes, 1988; Fig. 1). In contrast to

* Corresponding author at: Department of Earth Sciences, Dalhousie University, 1355 Oxford Street, Halifax, NS B3A 0B1, Canada.
E-mail address: j.evan@dal.ca (J. Evangelatos).
[1] Present address: Center for Coastal and Ocean Mapping, University of New Hampshire, 24 Colovos Road, Durham, NH, 03824, USA.
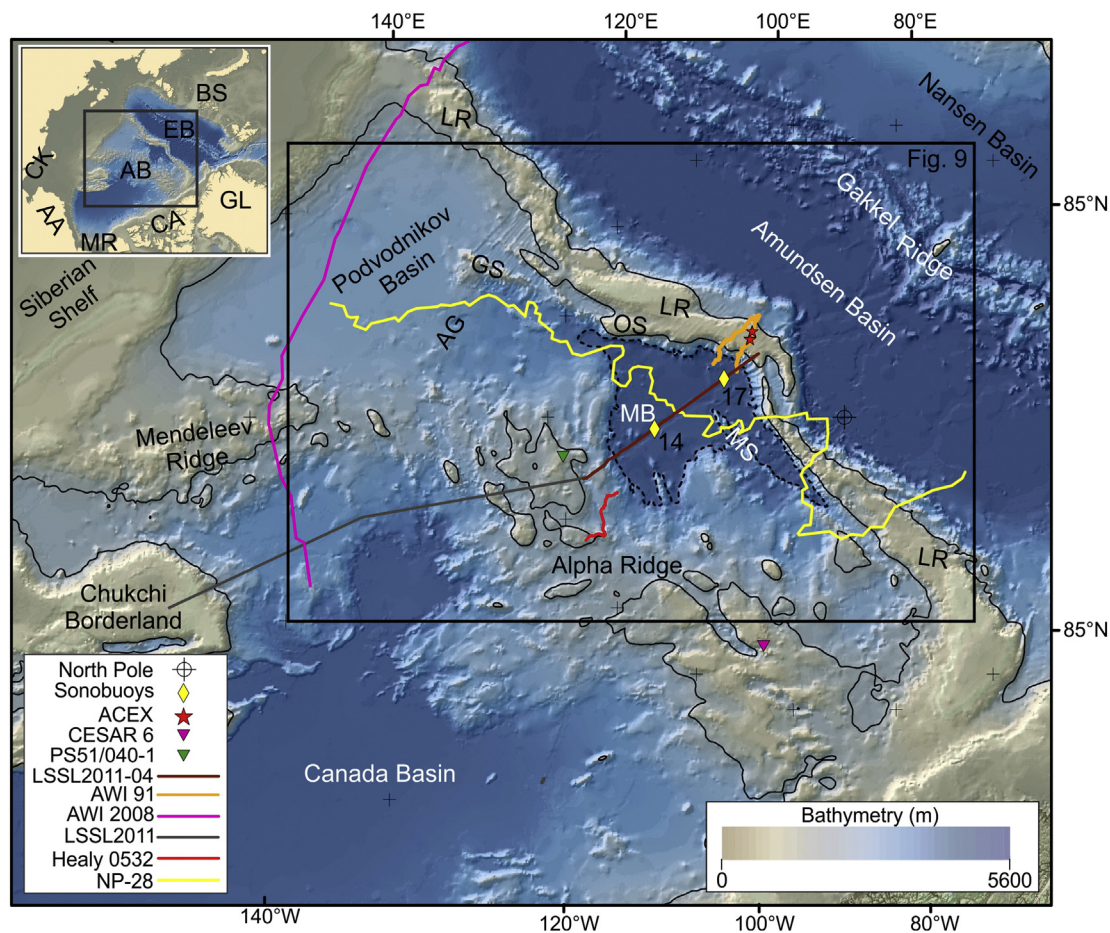
Fig. 1. Colour-shaded bathymetric map of northern Amerasia and Eurasia basins. Makarov Basin is delineated by a dashed line representing the 3700 m bathymetric contour. The thin black like corresponds with the 2000 m bathymetric contour, which is used to describe Lomonosov Ridge. Acronyms used in this figure and others are: AA — Arctic Alaska, AB — Amerasia Basin, AG — Arlis Gap, BS — Barents Shelf, CA — Canadian Arctic margin, CK — Chukotka, EB — Eurasia Basin, GL — Greenland, GS — Geophysicists Spur, LR — Lomonosov Ridge, MB — Makarov Basin, MR — Mackenzie River delta, MS — Marvin Spur, OS — Oden Spur. Note, the name Geophysicists Spur is not officially included in the General Bathymetric Chart of the Oceans Gazetteer (http://www.gebco.net/), but we use it as it is common in the Russian literature (e.g. Morozov et al., 2013; Taldenkova et al., 2014). Other studies shown in this figure are: ACEX [drill sites from IODP Expedition 302; Backman et al., 2006], CESAR 6 [piston core; Mudie and Blasco, 1985], PS51/040-1 [sediment core; Jokat, 1999], AWI 91 [MCS; Jokat et al., 1992, 1995], AWI 2008 [MCS; Weigelt et al., 2014], Healy 0532 [MCS; Bruvoll et al., 2010], LSSL2011 [MCS; Mosher, 2012], NP-28 [seismic reflection from ice-station; Langinen et al., 2009]. Map projection is North Pole Stereographic with a latitude of origin of 75° N and a central meridian of 90° W. Bathymetry and elevation are from the International Bathymetric Chart of the Arctic Ocean (IBCAO), version 3.0 (Jakobsson et al., 2012).

Eurasia Basin, the geological history of Amerasia Basin is not well known. This uncertainty results largely from the paucity of data in Amerasia Basin, which is due to its remote location and perennial cover of sea ice, and due to the geological complexity of the region. Furthermore, plate-reconstructions of the basin are hampered by the absence of well-defined magnetic isochron anomalies (Gaina et al., 2011). Consequently, opposing models for the genesis of Amerasia Basin have been advanced (cf. Miller and Verzhbitsky, 2009; Grantz et al., 2011). Unravelling the history of Makarov Basin, which lies in the underexplored northern Amerasia Basin, will support interpretation of the tectonic origin of the entire Amerasia Basin and its post-formation history. The objective of this study, therefore, is to decipher the tectonic and sedimentological history of northern Amerasia Basin by analysing the stratigraphy, structure and morphology of Makarov Basin and surrounding regions using recently acquired seismic reflection and bathymetric data.

2. Geological setting

Makarov Basin lies at the northern extent of Amerasia Basin between Alpha Ridge and Lomonosov Ridge (Fig. 1). The basin encompasses an area of approximately 63,000 km^2 and its abyssal plain reaches depths of 4000 m (Fig. 1). Lomonosov Ridge is reasonably well-understood to

be a continental fragment isolated by opening of Eurasia Basin in the Cenozoic (Rowley and Lottes, 1988; Jackson et al., 2010). The Eurasian margin of Lomonosov Ridge is thus conjugate to the Barents Shelf margin. On the opposite side, Geophysicists, Oden and Marvin spurs are linear ridges that trend sub-parallel to Lomonosov Ridge (Fig. 1). These features are interpreted as continental fragments splintered off of Lomonosov Ridge (Cochran et al., 2006).

Alpha Ridge forms the southern border of Makarov Basin. The Alpha and Mendeleev ridges are part of a large igneous province (LIP), as evidenced by its high amplitude magnetic anomalies (Weber, 1986; Vogt et al., 2006), velocity structure (Funck et al., 2011), and basalts recovered in situ (Van Wagoner et al., 1986; Andronikov et al., 2008; Jokat, 1999). Together with Cretaceous volcanic suites found throughout the circum-Arctic (e.g. Hansen Point volcanics on Ellesmere Island; Estrada and Henjes-Kunst, 2004), the Alpha–Mendeleev ridge complex is assumed to be part of the greater High Arctic Large Igneous Province (HALIP) (Maher, 2001; Tegner et al., 2011). The duration of the HALIP and its timing relative to the opening of Amerasia Basin are disputed (Estrada, 2015). There is also current debate about whether the Alpha–Mendeleev ridge complex is an oceanic plateau emplaced on top of oceanic crust (e.g. Funck et al., 2011; Jokat et al., 2013), or stretched continental crust overprinted by later magmatism (e.g. Lebedeva-Ivanova et al., 2006; Døssing et al., 2013). The distinct
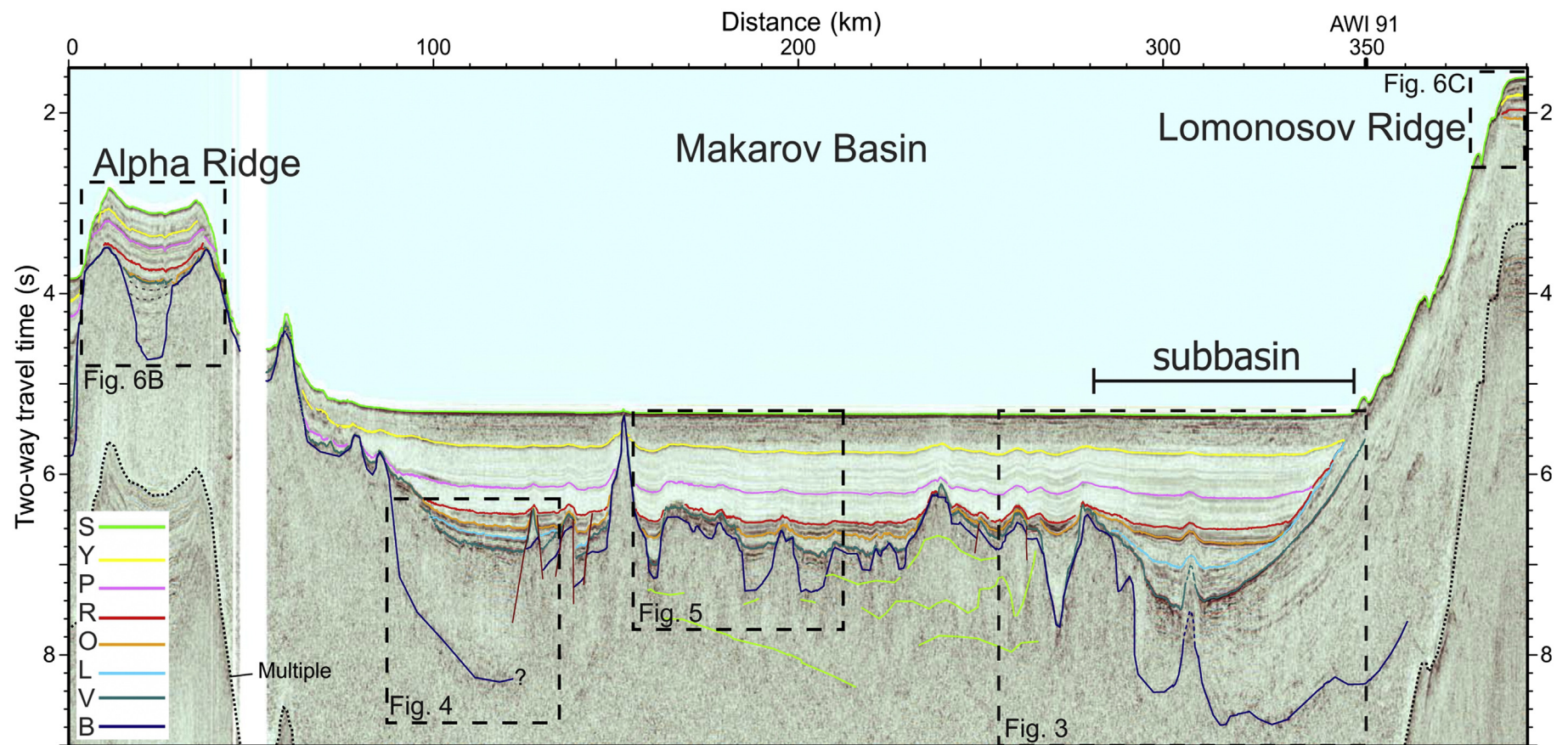
Fig. 2. MCS profile of line LSSL2011-04 is shown in the depth domain. Seafloor multiple is outlined by dotted black line. Lime green lines represent isolated semi-coherent acoustic signal within acoustic basement. Brown lines are for faults. The trackline of the profile is plotted in Fig. 1. Time sections shown in Figs. 3–6 are outlined by dashed boxes.

Table 1
Seismic horizons are described from deepest to shallowest. Listed depths are for the abyssal part of Makarov Basin between 80 and 352 km. Abrupt changes due to structural highs along horizon **B** are excluded.

Horizon	Colour	Description
B	Dark blue	Delineates amorphous acoustic signal (Facies 1) from overlying coherent seismic facies, thus defining the top of acoustic basement.
V	Dark cyan	A distinct high amplitude reflection easily discerned in Makarov Basin, but less so beneath the ridges. The **V** horizon clearly demarcates a relatively continuous and stratified section from an underlying section characterized by semi-coherent signal (Facies 2).
L	Light blue	Defined by an up section change from Facies 4 to Facies 5 with the latter onlapping against this horizon. It is mapped in two separate locations along the line: 99 to 133 km, and 286 to 329 km.
O	Orange	Observed at the base of a band of prominent basin-wide reflections (Facies 6). The depth of this reflection is 6.30–6.74 s TWTT.
R	Red	Delineates the top of the band of reflections discussed under the **O** horizon. The **R** horizon is not always well constrained due to gradational weakening of amplitude strength with decreasing depth. This reflection is mostly constrained between 6.27–6.60 s TWTT.
P	Pink	A high amplitude reflection that parallels the **R** horizon and spans the length of Makarov Basin at a depth of approximately 5.71–6.26 s TWTT (except where it intersects structural highs or on the flanks of Alpha and Lomonosov ridges).
Y	Yellow	Similar to the **P** horizon, but generally found at approximate depths of 5.28–5.79 s TWTT. This horizon is embedded between relatively disrupted reflections (Facies 8).
S	Green	Seafloor reflection.

magnetic character of the Alpha–Mendeleev ridge complex extends under Makarov Basin (Saltus et al., 2011). Isolated bedrock elevations found in the southeastern part of Makarov Basin are considered to be genetically related to Alpha Ridge (Jackson et al., 1986).

Although there are many tectonic models explaining the creation of the early Arctic Ocean (i.e. Amerasia Basin), the "rotational" model is the most widely accepted (e.g. Carey, 1958; Tailleur, 1973; Grantz et al., 1979, 1998, 2011). According to this model, the Arctic Alaska–Chukotka microplate rifted and drifted away from the Canadian Arctic continental margin about a pole of rotation located in the Mackenzie River delta region (Lawver et al., 2002). Spreading is thought to have commenced in the Early Cretaceous (Embry and Dixon, 1994), although

the age is not well constrained. The rotational model was buoyed by the discovery of a negative gravity anomaly that bisects Canada Basin. It was interpreted as a buried extinct spreading centre (Laxon and McAdoo, 1994) and negative basement relief coincident with this gravity anomaly has since been resolved by seismic reflection (Mosher et al., 2012). The gravity anomaly is not observed within the Alpha–Mendeleev LIP magnetic domain (Saltus et al., 2011), suggesting that any previous existing basement structure is masked by late magmatism related to the Alpha–Mendeleev ridge complex. Consequently, the northern extent of spreading and the nature of the margin between Amerasia Basin and Lomonosov Ridge are ambiguous and the tectonics are not well constrained.
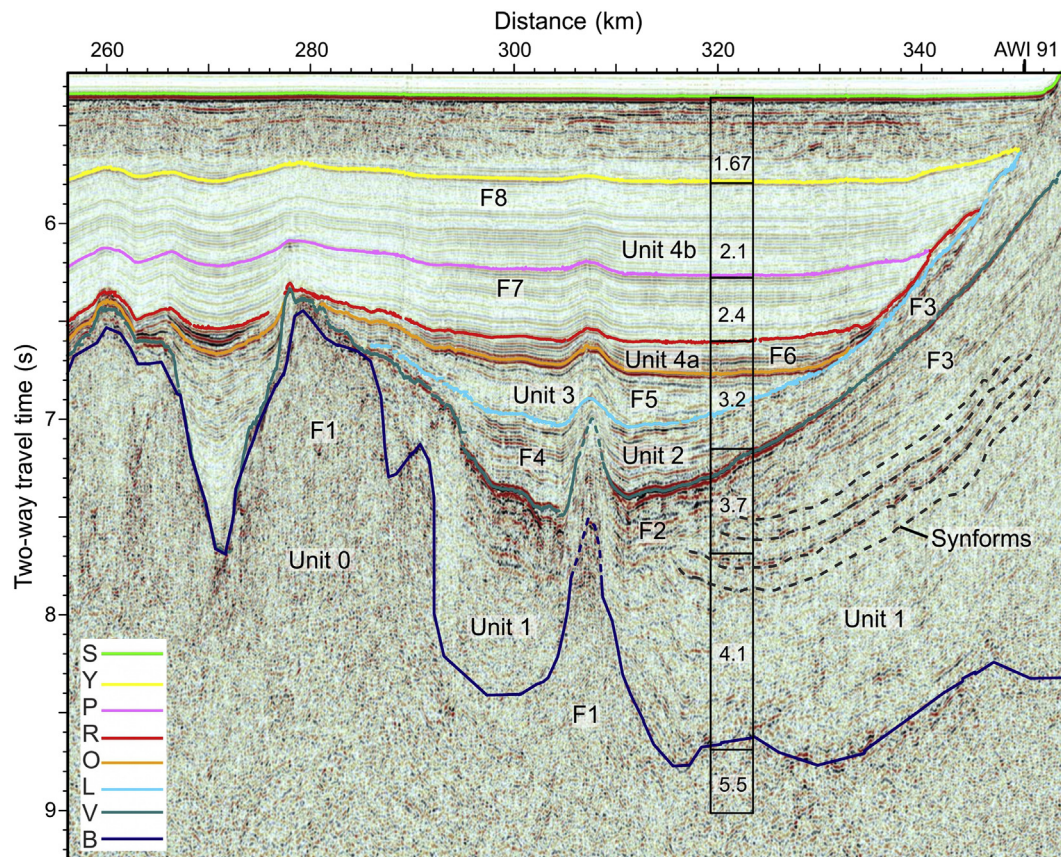

Fig. 3. A section of line LSSL2011-04 outlining the deep subbasin is shown. Dashed black lines mark synformal reflections. Data from sonobuoy SB2011-17 are used for calculating the P-wave interval velocities (km·s^{-1}) shown in the column (Chian and Lebedeva-Ivanova, 2015). Seismic facies are described under Section 4.2.
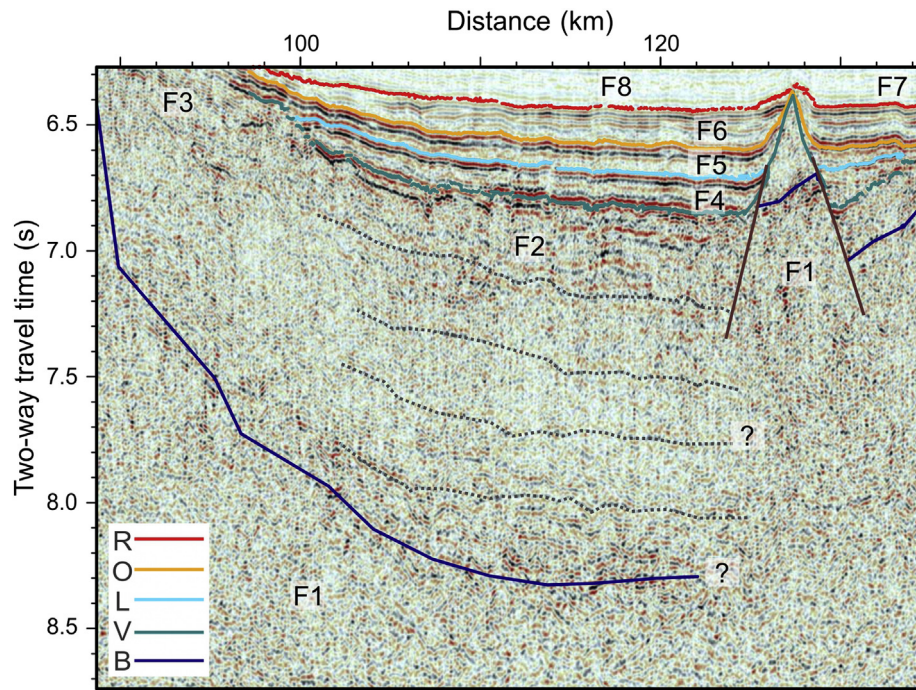
Fig. 4. A section of line LSSL2011-04 near Alpha Ridge is shown. Dotted black lines mark semi-coherent reflections in Unit 1. Seismic facies are described under Section 4.2.

3. Methodology

3.1. Data acquisition

Multi-channel seismic (MCS) reflection data used in this study were acquired in 2011 as part of a Canadian-American collaboration using two ice breakers: the Canadian Coast Guard Ship *Louis S. St-Laurent* and the US Coast Guard Cutter *Healy* (Mosher, 2012; Mayer and Armstrong, 2011). The *Healy* broke ice ahead of the *Louis S. St-Laurent* during seismic operations. The seismic source consisted of a cluster of three *Sercel* GI guns with a combined volume of 1150 in^3. The array was towed 11.5 m below the sea surface (below the depth of sea ice) and tight against the stern of the ship to protect it from ice. The receiver was a 230 m-long hydrophone streamer and the active section consisted of 16 channels spaced 6.25 m apart. Each channel comprised a group of four hydrophones. The signature of the seismic source yielded a peak power frequency at 45 Hz. Assuming a constant water velocity of 1500 m s^{-1}, the corresponding vertical resolution of the seismic data is ~8 m (assuming the Rayleigh criteria of 1/4 wavelength as detectable resolution). Horizontal resolution is limited by the shot interval and post-stack trace interval. The shot interval was variable because firing was based on time, not distance. Post-stack trace spacing is nominally 25 m. Details of the acquisition system are found in Mosher et al. (2009) and Mosher (2012).

3.2. Seismic processing and interpretation

Details of the seismic processing are provided by Shimeld (2009, 2011). Fig. 2 shows the final processed version of the seismic reflection data. Processed SEG-Y files, including geographic position data, were imported into *IHS Kingdom Suite* seismic interpretation software. Seismic reflection horizons were then mapped/picked based on peak amplitudes. Processed seismic data are sampled at 4 ms (i.e. 6 m at 1500 m s^{-1}), thus the best interpretation resolution is close to the Rayleigh resolution of the seismic data. Vertical offsets indicative of faulting were also mapped. Picked seismic horizons were converted to depth using seismic velocities derived from refraction analysis reported in Chian and Lebedeva-Ivanova (2015). These sonobuoys were

deployed during acquisition of the seismic reflection data (see Mosher, 2012) and, therefore, coincide precisely with the MCS profile.

4. Results

The 2011 seismic line LSSL2011-04 is a 400 km-long transect across Makarov Basin from Alpha Ridge in the south to Lomonosov Ridge in the north (Figs. 1 and 2). The sedimentary section was interpreted by correlating eight seismic reflection horizons and eight seismic facies that were subsequently organized into five seismic units.

4.1. Seismic horizons

The eight picked seismic reflection horizons are labelled B, V, L, O, R, P, Y and S from bottom to top in Fig. 2. They represent prominent laterally continuous horizons or horizons of significant change in reflection characteristics (Table 1). With the exception of horizons P and Y, seismic horizons demarcate boundaries of different seismic facies assemblages.

4.2. Seismic facies

Seismic facies defined along line LSSL2011-04 are presented in Figs. 3, 4, 5, and 6, and described below:

- Facies 1 (F1) represents an amorphous acoustic facies with little coherent energy. Any hint of coherent energy may represent structure, but could also result from multi-path echo returns.
- Facies 2 (F2) consists of bands of reflections with limited lateral continuity (<15 km) featuring medium coherency and low frequencies with high amplitudes that attenuate rapidly with increasing depth. These attributes are highly variable and individual reflections within a specific band may diverge or remain parallel and concordant with an upper boundary.
- Facies 3 (F3) comprises low to medium amplitude reflections that dip basinward. The reflections are moderately coherent and contorted upslope.
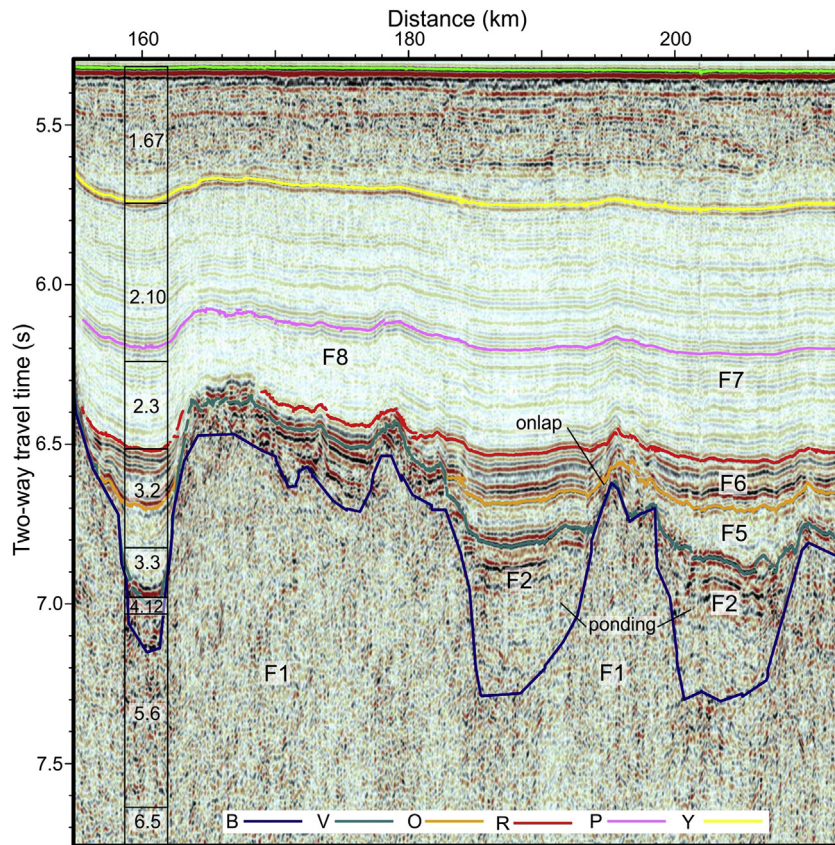- Facies 4 (F4) is defined by stratified reflections with medium to high

Fig. 5. A section of line LSSL2011-04 is shown depicting bands of layered reflections immediately beneath the V horizon. These reflections appear to be ponding in areas of negative relief. Data from sonobuoy SB2011-14 are used for calculating the P-wave interval velocities (km·s^{-1}) shown in the column (Chian and Lebedeva-Ivanova, 2015). Seismic facies are described under Section 4.2.

amplitudes. Reflections are higher in frequency and are more continuous in comparison with Facies 2. In addition, reflections are crudely concordant with the lower boundary.

• Facies 5 (F5) is represented by stratified reflections with low to medium coherency and amplitude strength. Lateral changes in amplitude characteristics are discerned and reflections are often tilted and/ or divergent.

• Facies 6 (F6) consists of a thin band of basin-wide continuous high amplitude reflections with lateral pinch-out terminations. Amplitude strength increases with depth. Reflections are generally concordant with underlying structures.

• Facies 7 (F7) is the most common seismic facies and consists of basin-wide continuous high frequency reflections that are stratified and concordant with underlying reflections. Reflection amplitudes are generally low to medium and vary laterally. Lateral coherency also varies.

• Facies 8 (F8) is similar to Facies 7, except that amplitudes are low and continuity is poor. Despite these characteristics, individual horizons trace across Makarov Basin.

4.3. Seismo-stratigraphic units

The eight seismic horizons and eight acoustic facies presented above were used to divide the seismic section into five seismic units. Seismic velocities used for estimating the thickness of units are shown in Figs. 3 and 4.

4.3.1. Unit 0 (Facies 1)

Unit 0 is generally composed of seismic Facies 1, which is incoherent signal. Isolated semi-coherent reflections are, however, distinguishable

(Fig. 2). The top of the unit, the **B** horizon, is a rugose surface with excursions in excess of 1 s two-way travel time (TWTT). Only one of these excursions reaches the seafloor at 152 km along the seismic profile (Fig. 2). The base of this unit is undefined.

4.3.2. Unit 1 (Facies 2 and 3)

Unit 1 consists of Facies 2 and 3 reflections. The base of the unit, the **B** horizon, is defined by high-amplitude and semi-coherent reflections that reach depths of 8.2 and 8.8 s TWTT near the Alpha and Lomonosov ridges, respectively (Fig. 2). Below the base of slopes, Facies 3 (basinward dipping reflections) grades laterally into Facies 2 or underlies it. Synformal deep reflections also appear truncated by Facies 2 (Fig. 3) near Lomonosov Ridge. Unit 1 is as much as 1800 ms TWTT (approximately 2.5–3 km) thick in the deep subbasin (Fig. 3) adjacent to the base of slope of this ridge. The dimensions of Unit 1 are not as clearly defined beneath the base of slope of Alpha Ridge, but semi-coherent reflections are identified (Fig. 4). Maximum thickness reaches 1400 ms TWTT — seismic velocities that would allow depth conversion are poorly constrained in this region. In Makarov Basin, the **B** horizon is commonly mapped along the base of bands of semi-coherent reflections (Facies 2) in sections of low relief. Lateral terminations suggest ponding beneath topographic lows of the **V** horizon (Fig. 5).

4.3.3. Unit 2 (Facies 3 and 4)

Facies 4 dominates in this unit, except on the flank of Lomonosov Ridge where Facies 3 (dipping reflections) is present. Similar to Unit 1, dipping reflections beneath the slope of Lomonosov Ridge (Facies 3) grade laterally into horizontal reflections (Facies 4). The basal contact shows abrupt truncations of reflections where relief on horizon **V** is rugged and downlap/onlap relationships where relief is smooth (Fig. 3). The **V** and **L** horizons are the bottom and top boundaries of Unit 2,
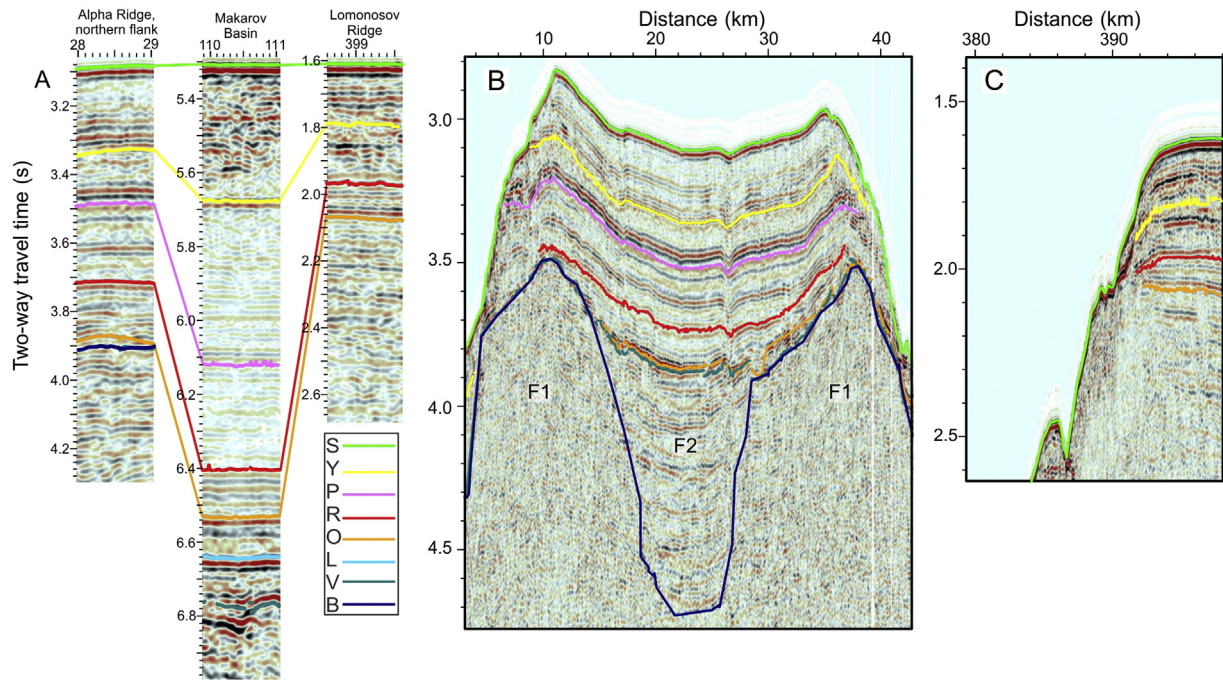
Fig. 6. Sections of line LSSL2011-04 showing A) seismo-stratigraphic correlation between Alpha Ridge, Makarov Basin and Lomonosov Ridge, B) and C) the sedimentary drape over Alpha Ridge and Lomonosov Ridge, respectively. Note ponding beneath the **V** horizon, in B). Seismic facies are described under Section 4.2.

respectively. The thickness of this unit is as much as 450 ms TWTT (750 m).

4.3.4. Unit 3 (Facies 5)

Unit 3 lies between the **L** horizon, or **V** if **L** is not present, at its base, and the **O** horizon at its top. It consists mainly of seismic Facies 5. Unit 3 is normally less than 280 ms TWTT (420 m) thick, except in a buried valley located between 266 and 277 km along line LSSL2011-04 (Fig. 3), where it reaches 1000 ms TWTT (1500 m). Its thickness strongly correlates with relief along the **B** or **V** horizons. Unit 3 reflections onlap against Unit 1 (where present), and are either truncated or lap against the **V** horizon (Fig. 5).

4.3.5. Unit 4 (Facies 6, 7 and 8)

The bottom and top boundaries of Unit 4 are horizons **O** and **S** (seafloor), respectively. This unit is further subdivided by the **R** horizon into a lower Unit 4a and an upper Unit 4b. In addition, horizons **P** and **Y** are embedded within the upper subunit. Units 4a and 4b generally range in thickness from 100 to 170 ms TWTT (120 to 200 m) for Unit 4a, and 640 to 920 ms TWTT (780 to 1000 m) for Unit 4b. Thicknesses are substantially less in sections of pronounced relief along the **V** horizon and at the edges of the basin. Seismic facies 6, 7 and 8 consist of stratified continuous reflections — amplitude strength and coherency distinguishing the three facies. Unit 4a consists exclusively of Facies 6. Facies 7 and 8 are interbedded within Unit 4b and also laterally grade into each other (Fig. 5). There is a conformable relationship between
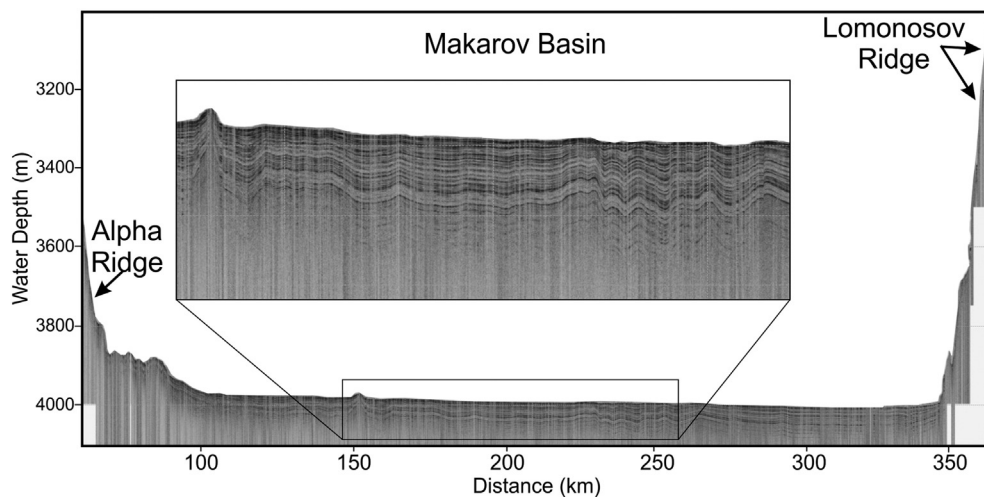

Fig. 7. Chirp subbottom profiler across Makarov Basin from Alpha Ridge (left) to Lomonosov Ridge (right). This line is coincident with the seismic line show in Fig. 2. Depth conversions were made assuming a water velocity of 1500 km s^{-1}.
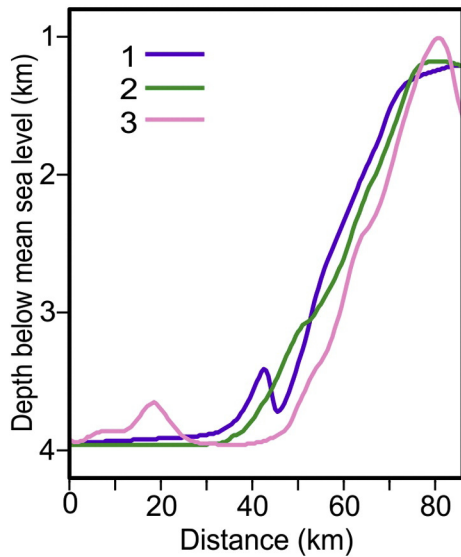
Fig. 8. Three bathymetric cross-sections from Makarov Basin (left) to Lomonosov Ridge (right) are shown. Location of lines shown in Fig. 9.

units 3 and 4. Reflections in this unit onlap against the edges of the basin. Evidence of major deformation is absent from this unit.

4.4. Alpha and Lomonosov ridges

Most seismic horizons mapped across Makarov Basin cannot be readily traced to the top of Alpha and Lomonosov ridges; reflections truncate at the edge of the basin or onlap and offlap the ridges resulting in pinch-out and condensed sections (Fig. 2). As a result, seismic reflection horizons were correlated between the ridges and Makarov Basin by matching reflection patterns (Fig. 6A).

On Alpha Ridge, ponding of Facies 2 reflections, beneath the **V** horizon, is observed between 16 and 30 km along the seismic profile (Fig. 6B). Shallow reflections, above the **O** horizon are concordant

with respect to underlying relief similar to Facies 7 and 8 of Makarov Basin. An erosional surface or post-depositional deformation are not observed in the shallow seismic section of Alpha Ridge.

Line LSSL2011-04 extends about 6 km over the crest of Lomonosov Ridge (Fig. 6C). Reflections below the **O** horizon are concordant with overlying reflections. Shallow reflections on Lomonosov Ridge are horizontal, except where they terminate at the ridge flank. The data show a thin drape on Lomonosov Ridge relative to Alpha Ridge.

4.5. Physiography

The seafloor of Makarov Basin is almost 4000 m deep, which is typically 200 m deeper than Canada Basin (Jakobsson et al., 2012). As revealed in high resolution subbottom profiler data (Chirp), the seafloor dips gently to the north on average (Fig. 7). The basin is about 300 km wide in a north–south direction and 400 km wide in its east to west orientation. Arlis Gap is a restricted connection with Podvodnikov Basin (Fig. 1). Unusual bends in the strike of Lomonosov Ridge near the point of the North Pole have long been recognized (Lane, 1997; Cochran et al., 2006). The bends offset the position of the top of Lomonosov Ridge from a straight line projection by more than 100 km and hosts an intra-ridge basin with a length of 140 km and a width of 25 km (Fig. 1). The segment of Lomonosov Ridge that is closer to North America appears blocky with a generally flat-lying crest that lies at depths of 500 to 1600 m and plunges northward. Minimum depths along the Siberian segment of the crest vary from 700 to 1700 m. For most of its length, the width of the Lomonosov Ridge varies from 50 km to 100 km between the 2000 m isobaths. Slopes along the Amerasian flank of Lomonosov Ridge are steep (4 to 8°), straight and laterally continuous (Fig. 8), as opposed to slopes on the Amundsen Basin-facing flank that appear segmented (i.e. not a continuous slope).

Marvin Spur is a small ridge feature that sub-parallels Lomonosov Ridge and extends into Makarov Basin. The minimum depth of Marvin Spur is ~1500 m. The spur plunges towards the centre of Makarov Basin where it disappears below sedimentary cover at 87.8° N and 176.1° E. The gap between Marvin Spur and Lomonosov Ridge narrows from 90 km near the centre of Makarov Basin to 30 km close to
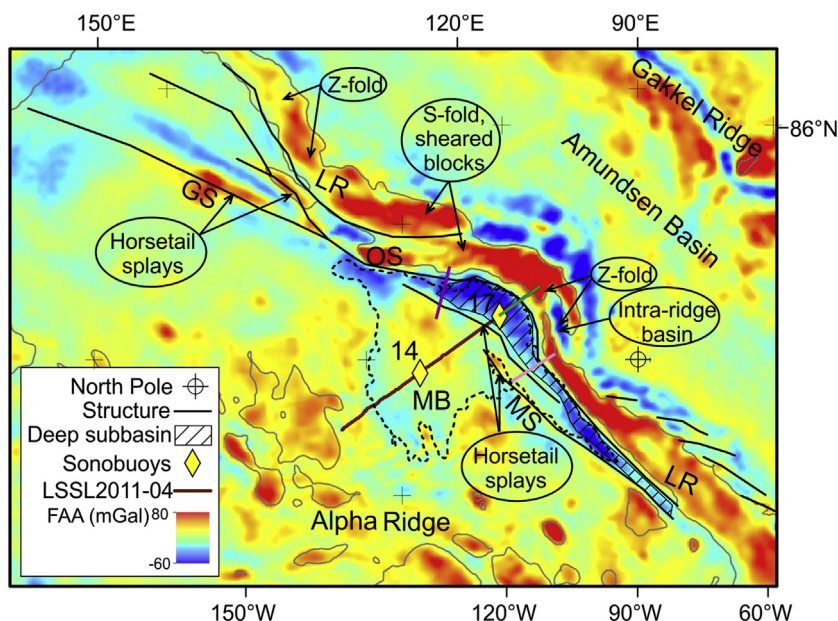

Fig 9. Colour-shaded free air anomaly (FAA) gravity map of Makarov Basin and surrounding areas is shown with structural interpretations overlain. Acronyms are defined in Fig. 1. The dashed black line and thin solid grey lines are the 3700 m and 2000 m bathymetric contours, respectively. Gravity values are from the compilation of Andersen et al. (2010).

the North American shelf. Towards the Siberian Shelf, Oden and Geophysicists spurs and other small ridges are observed *fanning out* of the Amerasian flank of Lomonosov Ridge (Fig. 1).

Alpha and Mendeleev ridges are as shallow as 1100 m water depth; nearly 2900 m above the abyssal plain of Makarov Basin. The width of Alpha Ridge is highly variable; in general, it narrows from 600 km near the Canadian Arctic margin to less than 200 km near Arlis Gap, where it abuts Mendeleev Ridge. Its length from the Canadian Arctic margin to the centre of the depression between Alpha and Mendeleev ridges is 1100 km. The morphology of Alpha Ridge is complex with many irregular ridges and troughs that are short in length (<150 km). The orientations of these features are crudely parallel to the overall trend of Alpha Ridge. Slopes from Alpha Ridge into Makarov Basin are highly variable but generally less steep than those from Lomonosov Ridge (< 6°).

5. Interpretations

5.1. Seismic interpretation

5.1.1. Unit 0
Unit 0 is part of the geological basement. This unit includes large volumes of magmatic material based on its acoustic characteristics (Facies 1), rugose nature of the top surface (horizon **B**) and proximity to the Alpha-Mendeleev ridge complex. Pinnacle-type structures that are part of this unit (e.g. 152 km along line; Fig. 2) are interpreted as volcanic edifices similar to those described in northern Canada Basin (Shimeld et al., 2016). We attribute the existence of these edifices to the Alpha–Mendeleev LIP. The nature of isolated semi-coherent energy in this unit is unclear, but we speculate that it represents lithological contacts of igneous origin (e.g. sills or volcanic layering), although it could be due to acoustic artefacts.

5.1.2. Unit 1
The stratified, high amplitude and semi-continuous character of Facies 2 reflections suggests that the upper part of this unit is composed of interbedded layers of volcanogenic and sedimentary material. The volcanogenic layers may represent volcanic flows, sills or volcanoclastic sediments, as they appear to infill low areas beneath horizon **V** (top of volcanics). Alternatively, their high amplitudes may result from post-depositional alteration. Sediment samples from similar acoustic horizons were recovered in 2010 from the top of a seamount in north-central Canada Basin by shallow coring (Edwards et al., 2010). Recovered material included hydrothermally altered sediments with high acoustic velocities. In this case, the high amplitude reflections may be due to hydrothermal alteration by warm fluids emanating from the underlying volcanics. In the deep subbasin (Fig. 3), Facies 3 reflections are interpreted as prograding slope sediments, agreeing with conclusions made by Kristoffersen et al. (2007) on the nearby AWI 91 lines (Fig. 1). Synformal reflections near the base of Lomonosov Ridge (Fig. 3) appear cross-cut by Facies 2 reflections, which suggest that those sediments were deposited during the early stage of opening of Makarov Basin. Unit 1 near Alpha Ridge is interpreted as a thick sequence of volcanic-dominated strata. Any sedimentary layers present are likely minor, as suggested by the poor coherency of corresponding reflections (Fig. 4).

5.1.3. Unit 2
Facies 3 of Unit 2, on the flank of Lomonosov Ridge, grades into Facies 4 within the deep subbasin adjacent to Lomonosov Ridge. As with Unit 1, these facies represent prograding slope sediments. Upslope contorted reflections of Facies 2 are indicative of slumping along the flank of Lomonosov Ridge, and are equivalent to the slump units that Kristoffersen et al. (2007) describe. Unit 2 is interpreted as being composed of slope and base of slope sediments.

5.1.4. Unit 3
Unit 3 infills many of the small basins formed by the dramatic basement relief. Faint reflections terminate laterally against units 0 or 1. Unit 3 reflections do not correlate to the flank of Lomonosov Ridge, but are rather concordant with underlying structure. These two characteristics suggest that sediments were deposited primarily by hemipelagic or pelagic processes.

5.1.5. Unit 4
Unit 4 is the thickest and most consistent sequence within Makarov Basin, accounting for the majority of the sedimentary stratigraphy. In Unit 4a, the higher amplitudes of Facies 6 reflections are attributed to changes in lithology as a result of possible turbidite deposition, or a siliceous phase of pelagic sedimentation. In Unit 4b, the stratified and concordant character of facies 7 and 8 are inferred to represent hemipelagic to pelagic sediments. The undulating nature of the seafloor and shallow sediments is also emphasized in the subbottom profiler data (Fig. 7), reflecting the topography of deeper structure.
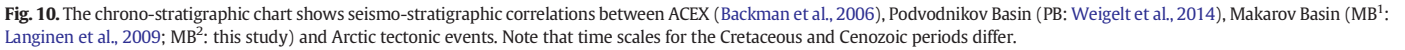
5.2. Alpha and Lomonosov ridges

Based on the interpretation that Alpha Ridge was heavily affected (if not created) by a large igneous province, the basement of the ridge is assumed to be dominantly composed of igneous material. Similar to Makarov Basin, Facies 2 on Alpha Ridge is interpreted as volcanics and/or volcanoclastics. On Lomonosov Ridge, reflections below the **O** horizon (Cenozoic–Mesozoic unconformity; Jokat et al., 1992) were interpreted as sedimentary successions of Mesozoic or older age (Jokat et al., 1992; Grantz et al., 2001). The drape sections of Alpha and Lomonosov ridges correlate with Unit 4 from Makarov Basin, and are similarly interpreted as pelagic to hemipelagic sedimentary strata.

5.3. Morphological and structural analysis

The flank of Lomonosov Ridge, dropping into Makarov Basin, forms a steep and straight slope (Fig. 8). This morphology contrasts with its opposite flank into Amundsen Basin which is block-faulted and stepped (Jokat et al., 1995; Cochran et al., 2006). This latter morphology is common to rifted passive margins (e.g. Scotian margin; Keen and Potter, 1995), while the straight steep flank into Makarov Basin is characteristic of transform or strike-slip margins (e.g. Lorenzo and Wessel, 1997; Basile and Allemand, 2002).

Another notable difference between the two flanks of Lomonosov Ridge is the existence of smaller sub-parallel ridges on the Amerasian side that are not present on the opposite side. A seismic reflection profile acquired along 81° N reveals buried basement horst" structures in Podvodnikov Basin that were interpreted as fragments of continental basement linked to the Lomonosov Ridge margin (Jokat et al., 2013). These structures are probably the buried extensions of Geophysicists Spur and other adjacent marginal ridges (cf. Figs. 1 and 9). Closer to the Canadian Arctic margin, line LSSL2011-04 reveals a buried structural high at ~280 km along the line (Fig. 3). Bathymetry, gravity and seismic crossings by ice-station NP-28 suggest that this basement structure is a distinct linear ridge between Marvin Spur and Lomonosov Ridge (Figs. 1 and 9; Figs. 3 and 5 in Langinen et al., 2009). Basile and Brun (1999) show that horsetail splays develop in the vicinity of the intersection between transform and divergent boundaries. Within the horsetail splay, block rotations about vertical and horizontal tilting axes lead to the formation of a surface slope perpendicular to the slope of the divergent basin, explaining the formation of tilted marginal ridges (e.g. Geophysicist Spur) at transform margins. In the context of our study, Geophysicists Spur, and nearby smaller ridges, and Marvin Spur, and its neighbouring ridges, are interpreted as two distinct sets of splay structures.

A distinguishing characteristic of Lomonosov Ridge is its prominent bends along its long axis (Figs. 1 and 9). The bend about the point of

Fig. 10. The chrono-stratigraphic chart shows seismo-stratigraphic correlations between ACEX (Backman et al., 2006), Podvodnikov Basin (PB: Weigelt et al., 2014), Makarov Basin (MB[1]: Langinen et al., 2009; MB[2]: this study) and Arctic tectonic events. Note that time scales for the Cretaceous and Cenozoic periods differ.

the North Pole forms a Z-fold. The segment of the ridge hosting an intra-ridge basin is adjacent to splay structures (Marvin Spur), and is, there-fore, interpreted as a releasing bend. Lomonosov Ridge then bends back, forming a S-fold centred on the segment where two flat-toped blocks appear sheared (near Oden Spur). This segment is interpreted as a restraining bend. The ridge then bends again before bending back to resume its original strike orientation. This last part is once more shaped like a Z-fold and is adjacent to splay structures (Geophysicists Spur and other small ridges), suggesting another releasing bend close to the Siberian Shelf (Fig. 9). The form of Lomonosov Ridge and the co-existence of extensional and compressional features along its Amer-asian flank imply dextral strike-slip deformation (Christie-Blick and Biddle, 1985; Basile and Brun, 1999; Noda, 2013).

The area between the basement structure (~280 km along line LSSL2011-04) and Lomonosov Ridge forms a deep narrow subbasin on seismic profile — deeper than the remainder of Makarov Basin (Fig. 2). The continuation of this subbasin is confirmed by multiple seismic crossings (e.g. Langinen et al., 2009) and its rhomboid shape is outlined by a gravity low (Fig. 9). This form is described by Mann et al. (1983); Basile and Brun (1999) and Noda (2013) as characteristic of pull-apart basins (grabens) in a transform margin setting. In addition, sandbox modelling of a transtensional system predicts the development of dual depocentres along the fault zone (Wu et al., 2009), which may be anal-ogous to the deep subbasin and the nearby intra-ridge basin (Fig. 9). Basile and Brun (1999) show that horsetail splays are also associated with pull-apart basins in large displacement transform settings.

The complex morphology of Alpha Ridge is (Fig. 1) is likely con-trolled by volcanic edifices (Vogt et al., 2006) and extension (Miller and Verzhbitsky, 2009; Bruvoll et al., 2010; Chernykh et al., 2015). It is not clear, however, if the troughs and ridges that characterize the morphology of Alpha Ridge are related to extensional/transtensional

stresses during formation of Makarov Basin, or if Alpha Ridge represents a later intrusion.

6. Discussion

6.1. Age model

Regional Arctic stratigraphies have been advanced for Lomonosov Ridge (Backman et al., 2006, 2008), Alpha and Mendeleev ridges (Bruvoll et al., 2010), Podvodnikov Basin (Weigelt et al., 2014) and Makarov Basin (Langinen et al., 2009)(seismic tracks shown in Fig. 1). In order to assign ages to our stratigraphy, we correlated seismic horizons with regional tectonic events and ACEX cores from the top of Lomonosov Ridge (Backman et al., 2006, 2008; Figs. 1 and 10). Line LSSL2011-04 crosses the AWI 91 lines, which were used to locate the ACEX drill sites, but only at the base of slope of Lomonosov Ridge. As such, the steep slope and thin sediment cover along the flank of the ridge make direct correlation speculative.

The age and affinity of basement (Unit 0) beneath Makarov Basin is not well constrained. According to the rotational model of Grantz et al. (2011), opening of Amerasia Basin, including Makarov Basin, com-menced about 195 Ma and was complete by 127.5 Ma. That would place a minimum age of 127.5 Ma for basement rocks within Makarov Basin, if they are original crust formed during creation of the basin. Alternatively, Døssing et al. (2013) interpreted magnetic anomalies close to the Canadian Arctic margin as seafloor spreading anomalies. According to their preferred reconstruction models, the oldest magnetic chrons in Makarov Basin in this area are between M16n and M11An.1n (~138–132 Ma) or M9n and M4n (~129–126 Ma) (Fig. 10). Embry and Dixon (1994) correlate the end of spreading with a regional

Cenomanian unconformity (100–93.9 Ma), assuming Makarov Basin formed contemporaneously with the rest of Amerasia Basin (Fig. 10).

The oldest sedimentary rocks of Makarov Basin are clastic sediments deposited on the slope and base of slope of the Mesozoic Barents Shelf (now Lomonosov Ridge), and preserved in units 1 and 2 (deep subbasin; Fig. 3). A network of channels on the Barents Shelf, such as exists today, likely supplied these sediments to the slope and to Makarov Basin prior to separation of Lomonosov Ridge from the Barents Shelf (Fig. 1). Indeed, the sedimentary record of the Barents Sea shows a drop in relative sea-level and the emergence of the Barents Shelf during the Late Cretaceous to Early Cenozoic (Faleide et al., 1993), providing a sediment source for the deep subbasin. The rest of Unit 1 is dominated by volcanogenic material, which we assume is related to emplacement of the Alpha–Mendeleev LIP. The minimum age of Unit 1, therefore, should coincide with the age of latest magmatism of the igneous province (Fig. 10). For this purpose, we rely on a basaltic sample retrieved at the top of volcanic rocks on adjacent Alpha Ridge (PS51/040-1; Fig. 1). Jokat et al. (2013) date this sample at 89 ± 1 Ma using $^{40}Ar/^{39}Ar$ isotopic dating techniques. This age nearly agrees with the 80 ± 2 Ma Rb/Sr age of Hansen Point volcanics found on nearby Ellesmere Island (Estrada and Henjes-Kunst, 2004).

Unit 2 sediments were also predominantly sourced from the Mesozoic Barents Shelf; thus, this unit predates rifting and formation of the Eurasia Basin. This source of sediment would be eliminated after separation of Lomonosov Ridge. Initial rifting possibly dates to the mid–Late Cretaceous (Drachev, 2011), or as late as 58 Ma (Glebovsky et al., 2006).

The base of Unit 3, horizon L, coincides with the end of the Barents Shelf as a source of sediment for Makarov Basin (Fig. 10). Langinen et al. (2009) do not identify the unconformity coincident with the change in sediment supply, probably due to the limited resolution of the NP-28 seismic line. This important marker is interpreted in the AWI 2008 data (Weigelt et al., 2014; Fig. 10); however, due to the proximity of the Siberian Shelf with their seismic track, the acoustic character of underlying (MB1) and overlying (MB2) units are markedly different from contemporaneous units from Makarov Basin.

The band of prominent reflections (Facies 6) that characterize Unit 4a is observed throughout the high Arctic Ocean (Weigelt et al., 2014). In the AWI 91 lines from Lomonosov Ridge (Fig. 1), this band of reflections is defined as seismic unit LR 3 (Jokat et al., 1995). The synthetic seismogram representing Unit 3 from the ACEX core matches well with LR 3 (Backman et al., 2008). Lithologically, Unit 3 is described as a silty clay interval hosting warm water microfossils (Moran et al., 2006) and spans from 56.2 to 49.7 Ma (Backman et al., 2008). Similar to the approach of Langinen et al. (2009), we jump-correlate the unit representing the band of prominent reflections with Unit 3 from ACEX (Fig. 10). The upper tens of metres of this core interval "contains silica that has been altered to cristobalite" (Moran et al., 2006). The base of ACEX Unit 3 is assumed to correlate with an erosional unconformity observed in the AWI lines (Jokat et al., 1995). It is not clear, however, if rocks immediately overlying this unconformity (hiatus) were sampled as recovery was not continuous between ACEX units 3 and 4 (Backman et al., 2006; Fig. 10). As such, the O horizon, base of Unit 4, is potentially older. Its assigned age does, however, approximately correspond with the initiation of spreading in Eurasia Basin (Glebovsky et al., 2006; Fig. 10).

The remaining sequence of Unit 4 is also jump correlated to ACEX units 1 and 2. The R horizon correlates with the base of ACEX Unit 2, which is biostratigraphically dated at 49.7 Ma (Backman et al., 2008). As recorded by the appearance of biosiliceous ooze, ACEX Unit 2 documents the transition to freshwater and relatively cool conditions in the Arctic Ocean (Moran et al., 2006). ACEX Unit 1 includes an Eocene to early Miocene hiatus (44.4–18.2 Ma). In Makarov Basin, the absence of a conspicuous basin-wide erosional surface at the appropriate depths and greater overall thickness of Unit 4 implies that sedimentation was continuous in Makarov Basin during this hiatus. Langinen et al. (2009)

similarly concluded that deposition was at least partly continuous in Makarov Basin during this period. Material eroded off of Lomonosov Ridge during this period may have deposited in Makarov Basin. Any contribution, however, would be relatively minor as there is no evidence of thick slope sequences during that time period. The P horizon is visible in the NP-28 line (see Fig. 10 in Langinen et al., 2009). We make no attempts to constrain the age of this reflection as the corresponding section in the ACEX borehole is absent. The Y horizon correlates with the base of ACEX Unit 1/5, indicating the end of the Eocene–early Miocene hiatus (Fig. 10). This period also coincides with the onset of enhanced water circulation and ventilated conditions in the Arctic Ocean (Jakobsson et al., 2007). Langinen et al. (2009) refer to this marker as "d_1". The undisturbed nature of Unit 4 sediments suggests that this layer was deposited after all major regional tectonic events ceased. Makarov Basin was, therefore, relatively tectonically inactive after the late Paleocene.

6.2. Implications for Amerasia Basin

6.2.1. Sedimentary history of Alpha Ridge

Seismic line Healy 0532 was acquired on the northern flank of Alpha Ridge in close proximity to our seismic profile (Bruvoll et al., 2010, 2012; Fig. 1). In agreement with our study, Bruvoll et al. (2012) concluded that the high amplitude reflections at or below basement at the Alpha and Mendeleev ridges (horizon V in this study) are caused by volcanic flows, sills and tuff. These layers are inferred to be responsible for the distinct high amplitude anomalies related to the Alpha–Mendeleev LIP (Vogt et al., 2006; Saltus et al., 2011).

The sedimentary cover over Alpha Ridge must be younger than ~90 Ma based on correlations with Makarov Basin (Fig. 6A) and ages from piston core CESAR 6 (Mudie and Blasco, 1985; Fig. 1). Unlike with Mendeleev Ridge (Bruvoll et al., 2012) and Lomonosov Ridge (Jokat et al., 1995), a planate surface is not present on Alpha Ridge according to line LSSL2011-04 (Fig. 6B) and the contiguous seismic line to the south (Brumley, 2014; Fig. 1). As such, the central part of Alpha Ridge was not emergent during the Cenozoic.

The inter-ridge stratigraphic correlation proposed in this study implies that the late Paleocene to early Miocene section (ACEX Unit 3 to base of Unit 1/5) is expanded on Alpha Ridge relative to Lomonosov Ridge. In contrast, the early Miocene to present succession (ACEX units 1/5 to 1/1) is similar in thickness between the two ridges (Fig. 11). The favoured of two age models (Model 2) advanced by Bruvoll et al. (2010) shows the early Eocene marker (base of ACEX
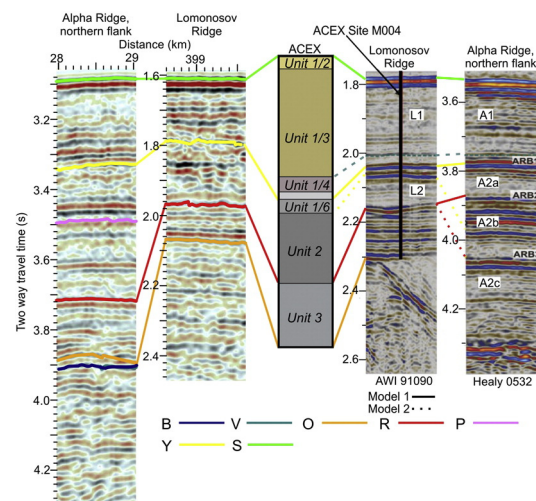

Fig. 11. Seismic sections of Alpha Ridge and Lomonosov Ridge from LSSL2011-04 (this study), AWI 91 and Healy 0532 (from Bruvoll et al., 2010) are correlated to ACEX and contrasted. Bruvoll et al. (2010) favoured Model 2 (dotted lines). ACEX column after Backman et al. (2008).

Unit 2) at similar depths to our study (horizon **R**). Their Model 2 does not mark the end of the major hiatus (base of ACEX *Unit 1/5*). Both the preferred model of Bruvoll et al. (2010) and the one proposed in this study agree that sedimentation was continuous on Alpha Ridge during the major hiatus (44.4–18.2 Ma) documented in ACEX core.

6.2.2. Amerasian margin of Lomonosov Ridge

Whether the Amerasian margin of Lomonosov Ridge was created by a transform (Cochran et al., 2006) or an Atlantic-style rift system (Langinen et al., 2009; Miller and Verzhbitsky, 2009) is debated. Evidence and interpretations presented above support a transform margin along the Amerasian flank of Lomonosov Ridge, consistent with the rotational model (Grantz et al., 1979, 1998, 2011; Lawver et al., 2002; Shephard et al., 2013). As supported by onshore geological studies in Arctic Russia, however, Miller and Verzhbitsky (2009) asserted that Makarov and Podvodnikov basins formed by rifting of the Lomonosov Ridge/Barents Shelf margin between ~120 and 105 Ma (Albian–Aptian). Also, Gaina et al. (2014) argued that the Late Cretaceous–Cenozoic position of stage poles for opening of the North Atlantic predicts extension perpendicular to Lomonosov Ridge for northern Amerasia Basin. To reconcile opposing explanations for the nature of the Amerasian flank of Lomonosov Ridge, we suggest the margin was initially transform and, as rotation continued, became transtensional and eventually extensional perpendicular to Lomonosov Ridge.

7. Conclusions

Makarov Basin of the central Arctic Ocean lies in a critical area to unravel the tectonic and sedimentological history of Amerasia Basin. Newly acquired seismic reflection data and the Arctic bathymetric chart were used to decipher the relationship between Makarov Basin, Alpha and Lomonosov ridges.

Five seismic reflection units describe the basement morphology and sedimentary history of Makarov Basin. The deepest unit (Unit 0) describes geological basement. Distinction of areas of original basement formed by extension and that formed or magmatically overprinted by the Alpha–Mendeleev LIP is not possible on seismic reflection data alone. Unit 1 is interpreted as mostly volcanogenic material, except in the deep subbasin (~5 km thick) adjacent to Lomonosov Ridge where a mix of volcanic and sedimentary layers is interpreted. The top of Unit 1 is a distinct basin-wide high amplitude reflection which is interpreted as a lithological transition from mixed volcanic and sedimentary rocks to sediment-dominated sequences. This horizon is dated to late-phase magmatism of the Alpha–Mendeleev LIP with a minimum age of ~89 Ma. The primary sediment source for units 1 and 2 is inferred to be the Mesozoic Barents Shelf. This source was disrupted after Lomonosov Ridge rifted from the Barents Shelf. This event may have begun as early as the mid-Late Cretaceous and rifting was complete by 58 Ma. Unit 3 and 4 are composed of hemipelagic to pelagic sediments that infill and drape over underlying structure. Even the topmost sediments reflect deeper surface morphologies indicating pelagic conditions have continued through to the present. These units indicate that Makarov Basin was isolated from sources of sediment by the surrounding Alpha and Lomonosov ridges, with little, if any, sediment sourced from these ridges after the mid-Late Cretaceous. The age of these units was determined by correlation with the ACEX core on Lomonosov Ridge. Similar to the Cenozoic section of Makarov Basin, the drape on Alpha and Lomonosov ridges were formed by pelagic to hemipelagic sedimentation. The significant hiatus in the ACEX core between 44 and 18.2 Ma is not apparent in the seismic reflection records of Makarov Basin or Alpha Ridge. The absence of a planate surface suggests that Alpha Ridge was not emergent during the Cenozoic.

The slope of Lomonosov Ridge into Makarov Basin is steep, straight and laterally continuous. The bend in Lomonosov Ridge forms half of a rhomboid shape adjacent to the deep subbasin within Makarov Basin. A number of ridges (e.g. Geophysicists, Oden and Marvin spurs),

found only on the Amerasian side, strike sub-parallel to Lomonosov Ridge. These features are interpreted as splay structures and bend in Lomonosov Ridge and the deep subbasin are characteristic of pull-apart basins. These features contrast with the stepwise and block-faulted form of the Amundsen Basin-facing flank of Lomonosov Ridge, which is known to be a classic rift margin. Instead, these features are characteristic of a transform/transtensional margin. This interpretation is consistent with the rotational model (e.g. Grantz et al., 2011). We suggest that the initial rotational spreading resulted in a transform/transtensional margin at Lomonosov Ridge (Mesozoic Barents Shelf margin). As spreading continued, the tectonic stress regime became extensional, perpendicular to Lomonosov Ridge. There is no evidence of extension later than the late Paleocene, as implied by the undisturbed character of Cenozoic strata in Makarov Basin.

References

Andersen, O.B., Knudsen, P., Berry, P., 2010. The DNSC08GRA global marine gravity field from double retracked satellite altimetry. J. Geod. 84. http://dx.doi.org/10.1007/s00190-009-0355-9.

Andronikov, A., Mukasa, S., Mayer, L.A., Brumley, K., 2008. First recovery of submarine basalts from the Chukchi Borderland and Alpha/Mendeleev Ridge, Arctic Ocean. Eos 89 (53), V41D–2124.

Backman, J., Jakobsson, M., Frank, M., Sangiorgi, F., Brinkhuis, H., et al., 2008. Age model and core-seismic integration for the Cenozoic Arctic Coring Expedition sediments from the Lomonosov Ridge. Paleoceanography 23, PA1S03. http://dx.doi.org/10.1029/2007PA001476.

Backman, J., Moran, K., McInroy, D.B., Mayer, L.A., Expedition 302 Scientists, 2006. Proceedings of the Integrated Ocean Drilling Program 302. http://dx.doi.org/10.2204/iodp.proc.302.101.2006.

Basile, C., Allemand, P., 2002. Erosion and flexural uplift along transform faults. Geophys. J. Int. 151, 646–653.

Basile, C., Brun, J.P., 1999. Transtensional faulting patterns ranging from pull-apart basins to transform continental margins: an experimental investigation. J. Struct. Geol. 21, 23–37.

Brozena, J.M., Childers, V.A., Lawver, L.A., Gahagan, L.M., Forsberg, R., Faleide, J.I., Eldholm, O., 2003. New aerogeophysical study of the Eurasia Basin and Lomonosov Ridge: implications for basin development. Geology 31, 825–828.

Brumley, K., 2014. Geologic Nature of the Chukchi Borderland, Arctic Ocean. Ph.D. Thesis, Stanford University, unpublished.

Bruvoll, V., Kristoffersen, Y., Coakley, B.J., Hopper, J.R., 2010. Hemipelagic deposits on the Mendeleev and northwestern Alpha submarine Ridges in the Arctic Ocean: acoustic stratigraphy, depositional environment and an inter-ridge correlation calibrated by the ACEX results. Mar. Geophys. Res. 31, 149–171.

Bruvoll, V., Kristoffersen, Y., Coakley, B.J., Hopper, J.R., Planke, S., Kandilarov, A., 2012. The nature of the acoustic basement on Mendeleev and northwestern Alpha ridges, Arctic Ocean. Tectonophysics 514, 123–145.

Carey, S.W., 1958. A tectonic approach to continental drift. In: Carey, S.W. (Ed.), Continental Drift; a Symposium, pp. 177–355 (Hobart, Tasmania).

Chernykh, A.A., Glebovsky, V.Y., Egorova, A.V., Redko, A.G., Suhanov, R.A., 2015. Tectonic structure and evolution of the Alpha–Mendeleev fracture zone. Abstract, The 7th International Conference on Arctic Margins, ICAM VII, Trondheim, Norway.

Chian, D., Lebedeva-Ivanova, N.N., 2015. Atlas of sonobuoy velocity analyses. Canada Basin, Geological Survey of Canada, Open File 7661 http://dx.doi.org/10.4095/295857 (55 pp.).

Christie-Blick, N., Biddle, K.T., 1985. Deformation and basin formation along strike-slip faults. In: Biddle, K.T., Christie-Blick, N. (Eds.), Strike-Slip Deformation, Basin Formation, and Sedimentation. Society Of Economic Paleontologists And Mineralogists, Special Publication 37, pp. 1–35.

Cochran, J.R., Edwards, M.H., Coakley, B.J., 2006. Morphology and structure of the Lomonosov Ridge, Arctic Ocean. Geochem. Geophys. Geosyst. 7, Q05019. http://dx.doi.org/10.1029/2005GC001114.

Døssing, A., Jackson, H.R., Matzka, J., Einarsson, I., Rasmussen, T.M., Olesen, A.V., Brozena, J.M., 2013. On the origin of the Amerasia Basin and the High Arctic Large Igneous Province—results of new aeromagnetic data. Earth Planet. Sci. Lett. 363, 219–230.

Drachev, S.S., 2011. Tectonic setting, structure and petroleum geology of the Siberian Arctic offshore sedimentary basins. In: Spencer, A. M., Embry, A. F., Gautier, D. L, Stoupakova, A. V., Sørensen, K. (Eds.), Arctic Petroleum Geology: Geol. Soc. London, Memoirs 35, pp. 364–394.

Edwards, B.D., Saint-Ange, F., Pohlman, J., Higgins, J., Mosher, D.C., Lorenson, T.D., Hart, P., 2010. Sedimentology of cores recovered from the Canada Basin of the Arctic Ocean. AGU Fall Meeting (Abs.) Vol. 1, p. 1915.

Embry, A., Dixon, J., 1994. The Age of Amerasia Basin. In: Thurston, D., Fujita, K. (Eds.), 1992 Proceedings International Conference on Arctic Margins. U.S. Department of the Interior Minerals Management Service Alaska Outer Continental Shelf Region (OCS Study MMS 94-0040), pp. 289–294.

Estrada, S., 2015. Geochemical and Sr–Nd isotope variations within cretaceous continental flood-basalt suites of the Canadian high arctic with a focus on the hassel formation basalts of northeast Ellesmere Island. Int. J. Earth Sci. 104, 1981–2005.

Estrada, S., Henjes-Kunst, F., 2004. Volcanism in the Canadian High Arctic related to the opening of the Arctic Ocean. Z. Dtsch. Geol. Ges. 154, 579–603.

Faleide, J.I., Vågnes, E., Gudlaugsson, S.T., 1993. Late Mesozoic-Cenozoic evolution of the south-western Barents Sea in a regional rift-shear tectonic setting. Mar. Pet. Geol. 10, 186–214.

Funck, T., Jackson, H.R., Shimeld, J., 2011. The crustal structure of the Alpha Ridge at the transition to the Canadian Polar Margin: results from a seismic refraction experiment. J. Geophys. Res. 116, B12101. http://dx.doi.org/10.1029/2011JB008411.

Gaina, C., Medvedev, S., Torsvik, T.H., Koulakov, I., Werner, S.C., 2014. 4D Arctic: a glimpse into the structure and evolution of the Arctic in the light of new geophysical maps, plate tectonics and tomographic models. Surv. Geophys. 35, 1095–1122.

Gaina, C., Werner, S.C., Saltus, R., Maus, S., 2011. Circum-Arctic mapping project: new magnetic and gravity anomaly maps of the Arctic. In: Spencer, A.M., Embry, A.F., Gautier, D.L., Stoupakova, A.V., Sørensen, K. (Eds.), Arctic Petroleum Geology. Geol. Soc. London, Memoirs 35, pp. 39–48.

Glebovsky, V.Y., Kaminsky, V.D., Minakov, A.N., Merkur'ev, S.A., Childers, V.A., Brozena, J.M., 2006. Formation of the Eurasia Basin in the Arctic Ocean as inferred from geohistorical analysis of the anomalous magnetic field. Geotectonics 40, 263–281.

Grantz, A., Clark, D.L., Phillips, R.L., Srivastava, S.P., Blome, C.D., Gray, L.B., Haga, H., Mamet, B.L., McIntyre, D.J., Mcneil, D.H., Mickey, M.B., Mullen, M.W., Murchey, B.I., Ross, C.A., Stevens, C.H., Silberling, N.J., Wall, J.H., Willard, D.A., 1998. Phanerozoic stratigraphy of Northwind Ridge, magnetic anomalies in the Canada basin, and the geometry and timing of rifting in the Amerasia basin, Arctic Ocean. GSA Bull. 110, 801–820.

Grantz, A., Eittreim, S., Dinter, D.A., 1979. Geology and tectonic development of the continental margin north of Alaska. Tectonophysics 59, 263–291.

Grantz, A., Hart, P.E., Childers, V.A., 2011. Geology and tectonic development of the Amerasia and Canada Basins, Arctic Ocean. In: Spencer, A.M., Embry, A.F., Gautier, D.L., Stoupakova, A.V., Sørensen, K. (Eds.), Arctic Petroleum Geology. Geol. Soc. London, Memoirs 35, pp. 771–799.

Grantz, A., Pease, V.L., Willard, D.A., Phillips, R.L., Clark, D.L., 2001. Bedrock cores from 89° north: implications for the geologic framework and Neogene paleoceanogragraphy of the Lomonosov Ridge and a tie to the Barents shelf. GSA Bull. 113, 1272–1281.

Jackson, H.R., Dahl-Jensen, T., the LORITA Working Group, 2010. Sedimentary and crustal structure from the Ellesmere Island and Greenland continental shelves onto the Lomonosov Ridge, Arctic Ocean. Geophys. J. Int. 182, 11–35. http://dx.doi.org/10.1111/j.1365-246X.2010.04604.x.

Jackson, H., Forsyth, D., Johnson, G., 1986. Oceanic affinities of the Alpha Ridge, Arctic Ocean. Mar. Geol. 73, 237–261.

Jakobsson, M., Backman, J., Rudels, B., Nycander, J., Frank, M., Mayer, L., Jokat, W., Sangiorgi, F., O'Regan, M., Brinkhuis, H., King, J., Moran, K., 2007. The early Miocene onset of a ventilated circulation regime in the Arctic Ocean. Nature 447, 986–990. http://dx.doi.org/10.1038/nature05924.

Jakobsson, M., Mayer, L., Coakley, B., Dowdeswell, J.A., Forbes, S., et al., 2012. The International Bathymetric Chart of the Arctic Ocean (IBCAO) Version 3.0. Geophys. Res. Lett. 39, L12609. http://dx.doi.org/10.1029/2012GL052219.

Jokat, W. (Ed.), 1999. ARCTIC '98: The Expedition ARK-XIV 1a of RV "Polarstern" in 1998. Berichte zur Polarforschung, AWI, Bremerhaven 308, p. 159 pp.

Jokat, W., Ickrath, M., O'Connor, J., 2013. Seismic transect across the Lomonosov and Mendeleev Ridges: Constraints on the geological evolution of the Amerasia Basin, Arctic Ocean. Geophys. Res. Lett. 40, 5047–5051.

Jokat, W., Uenzelmann-Neben, G., Kristoffersen, Y., Rasmussen, T., 1992. ARCTIC'91: Lomonosov Ridge—a double sided continental margin. Geology 20, 887–890.

Jokat, W., Weigelt, E., Kristoffersen, Y., Rasmussen, T., Schöne, T., 1995. New insights into the evolution of the Lomonosov Ridge and the Eurasian Basin. Geophys. J. Int. 122, 378–392.

Keen, C.E., Potter, P., 1995. Formation and evolution of the Nova Scotian rifted margin: evidence from deep seismic reflection data. Tectonics 14, 918–932.

Kristoffersen, Y., Coakley, B.J., Hall, J.K., Edwards, M., 2007. Mass wasting on the submarine Lomonosov Ridge, central Arctic Ocean. Mar. Geol. 243, 132–142.

Lane, L.S., 1997. Canada Basin, Arctic Ocean: evidence against a rotational origin. Tectonics 16, 363–387.

Langinen, A.E., Lebedeva-Ivanova, N.N., Gee, D.G., Zamansky, Y.Y., 2009. Correlations between the Lomonosov Ridge, Marvin Spur and adjacent basins of the Arctic Ocean based on seismic data. Tectonophysics 472, 309–322.

Lawver, L.A., Grantz, A., Gahagan, L.M., 2002. Plate kinematic evolution of the present Arctic region since the Ordovician. Special Paper-Geol. Soc. Am. 360, pp. 333–358

Laxon, S., McAdoo, D., 1994. Arctic Ocean gravity field derived from ERS-1 satellite altimetry. Science 265, 621–624.

Lebedeva-Ivanova, N.N., Zamansky, Y., Langinen, A., Sorokin, M., 2006. Seismic profiling across the Mendeleev Ridge at 82°N: evidence of continental crust. Geophys. J. Int. 165, 527–544.

Lorenzo, J.M., Wessel, P., 1997. Flexure across a continent–ocean fracture zone: the northern Falkland/Malvinas Plateau, South Atlantic. Geo-Mar. Lett. 17, 110–118.

Maher Jr., H.D., 2001. Manifestations of the Cretaceous High Arctic large igneous province in Svalbard. J. Geol. 109, 91–104.

Mann, P., Hempton, M.R., Bradley, D.C., Burke, K., 1983. Development of pull-apart basins. J. Geol. 91, 529–554.

Mayer, L.A., Armstrong, A.A., 2011. US Law of the Sea cruise to map the foot of the slope and 2500-m isobath of the US Arctic Ocean margin. (<http://ccom.unh.edu/theme/law-sea/cruise-reports/arctic. > (last accessed 06.05.14.)).

Miller, E.L., Verzhbitsky, V., 2009. Structural studies in the Pevek region, Russia: implications for the evolution of the East Siberian Shelf and Makarov Basin of the Arctic Ocean. Stephan Mueller Publication Series 4, pp. 223–241.

Moran, K., Backman, J., Brinkhuis, H., Clemens, S.C., Cronin, T., et al., 2006. The Cenozoic palaeoenvironment of the Arctic Ocean. Nature 441, 601–605.

Morozov, A.F., Petrov, O.V., Shokal'skiy, S.P., Kashubin, S.N., Kremenetskiy, A.A., Shkatov, M.Yu, Kaminsky, V.D., Gusev, E.A., Grikurov, G.E., Rekant, P.V., Shevchenko, S.S., Sergeev, S.A., Shatov, V.V., 2013. New geological data are confirming continental origin of the Central Arctic Rises. Reg. Geol. Metallogeny 53, 34–55.

Mosher, D.C., 2012. 2011 Canadian High Arctic seismic expedition: CCGS Louis S. St-Laurent expedition report. Geological Survey of Canada, Open File 7053 (290 pp.).

Mosher, D.C., Shimeld, J., Hutchinson, D.R., 2009. 2009 Canada Basin seismic reflection and refraction survey, western Arctic Ocean: CCGS Louis S. St-Laurent expedition report. Geological Survey of Canada, Open File 6343 (266 pp.).

Mosher, D.C., Shimeld, J., Hutchinson, D., Chian, D., Lebedova-Ivanova, N., Jackson, H.R., 2012. Canada Basin revealed. Arctic Technology Conference OTC 23797.

Mudie, P.J., Blasco, S.M., 1985. Lithostratigraphy of the CESAR Cores. In: Jackson, H.R., Mudie, P.J., Blasco, S.M. (Eds.), Initial Geological Data Report on CESAR, The Canadian Expedition to Study the Alpha Ridge, Arctic Ocean. Geological Survey of Canada, Ottawa, Geological Survey of Canada Paper 84–22, pp. 59–99.

Noda, A., 2013. Strike-slip basin — its configuration and sedimentary facies. In: Itoh, Y. (Ed.), Mechanism of SEDIMENTARY basin Formation — Multidisciplinary Approach on Active Plate Margins. InTech, pp. 28–57.

Rowley, D.B., Lottes, A.L., 1988. Plate-kinematic reconstructions of the North Atlantic and Arctic: late Jurassic to present. Tectonophysics 155, 73–120.

Saltus, R.W., Miller, E.L., Gaina, C., Brown, P.J., 2011. Regional magnetic domains of the Circum-Arctic: a framework for geodynamic interpretation. In: Spencer, A.M., Embry, A.F., Gautier, D.L., Stoupakova, A.V., Sørensen, K. (Eds.), Arctic Petroleum geology. Geol. Soc. London, Memoirs 35, pp. 49–60.

Shephard, G.E., Müller, R.D., Seton, M., 2013. The tectonic evolution of the Arctic since Pangea breakup: integrating constraints from surface geology and geophysics with mantle structure. Earth Sci. Rev. 124, 148–183. http://dx.doi.org/10.1016/j.earscirev.2013.05.012.

Shimeld, J., 2009. Chapter 5: acquisition and processing of the seismic reflection data. In: Mosher, D.C., Shimeld, J.W., Hutchinson, D.R. (Eds.), 2009 Canada Basin Seismic Reflection and Refraction Survey, Western Arctic Ocean: CCGS Louis S. St-Laurent Expedition Report, Geological Survey of Canada, Open File 6343, pp. 151–171.

Shimeld, J., 2011. Chapter 2: acquisition and processing of the seismic reflection data. In: Mosher, D.C., Shimeld, J.W., Chapman, C.B. (Eds.), 2010 Canada Basin Seismic Reflection and Refraction Survey, Western Arctic Ocean: CCGS Louis S. St-Laurent Expedition Report, Geological Survey of Canada, Open File 6720, pp. 49–68.

Shimeld, J., Li, Q., Chian, D., Lebedeva-Ivanova, N.N., Jackson, H.R., Mosher, D.C., Hutchinson, D.R., 2016. Seismic velocities within the sedimentary succession of the Canada Basin and southern Alpha–Mendeleev Ridge, Arctic Ocean: evidence for accelerated porosity reduction? Geophys. J. Int. 204, 1–20.

Srivastava, S.P., 1985. Evolution of the Eurasian Basin and its implication to the motion of Greenland along Nares Strait. Tectonophysics 114, 29–53.

Taldenkova, E., Nikolaev, S., Rekant, P., Chistyakova, N., 2014. Pleistocene sediment sequence of the southern Lomonosov Ridge, Arctic Ocean: preliminary stratigraphic subdivision based on iceberg-rafted debris and benthic foraminiferal records. In STRATI 2013. Springer International Publishing, pp. 1321–1325.

Tailleur, I.L., 1973. Probable rift origin of Canada basin, Arctic Ocean. In: Pitcher, M.G. (Ed.), Arctic geology. American Association of Petroleum Geologists Memoir 19, pp. 526–535.

Tegner, C., Storey, M., Holm, P.M., Thorarinsson, S.B., Zhao, X., Lo, C.H., Knudsen, M.F., 2011. Magmatism and Eurekan deformation in the High Arctic Large Igneous Province: $^{40}Ar-^{39}Ar$ age of Kap Washington Group volcanics, North Greenland. Earth Planet. Sci. Lett. 303, 203–214.

Van Wagoner, N.A., Williamson, M.-C., Robinson, P.T., Gibson, I.L., 1986. First samples of acoustic basement recovered from the Alpha Ridge, Arctic Ocean: new constraints for the origin of the ridge. J. Geodyn. 6, 177–196.

Vogt, P.R., Jung, W.-Y., Jakobsson, M., Mayer, L., Williamson, M., 2006. The Alpha–Mandeleev magmatic province, Arctic Ocean — a new synthesis. Eos 87, 36 (Abs.).

Vogt, P.R., Taylor, P.T., Kovacs, L.C., Johnson, G.L., 1979. Detailed aeromagnetic investigations of the Arctic Basin. J. Geophys. Res. 84, 1071–1089.

Weber, J.R., 1986. The Alpha Ridge: gravity, seismic and magnetic evidence for a homogenous, mafic crust. J. Geodyn. 6, 117–136.

Weigelt, E., Franke, D., Jokat, W., 2014. Seismostratigraphy of the Siberian Arctic Ocean and adjacent Laptev Sea Shelf. J. Geophys. Res. 119, 5275–5289. http://dx.doi.org/10.1002/2013JB010727.

Wu, J., McClay, K., Whitehouse, P., Dooley, T., 2009. 4D analogue modelling of transtensional pull-apart basins. Mar. Pet. Geol. 26, 1608–1623.